Inorganic Chemistry

pubs.acs.org/IC

Article

Tetraphenylethylene(TPE)-Containing Metal–Organic Nanobelt and Its Turn-on Fluorescence for Sulfide (S^{2-})

Kaixiu Li,[#] Zhengguang Li,[#] Die Liu,[*] Mingzhao Chen, Shi-Cheng Wang, Yi-Tsu Chan, and Pingshan Wang[*]

Cite This: https://dx.doi.org/10.1021/acs.inorgchem.0c00928

Read Online

ACCESS | Metrics & More | Article Recommendations | Supporting Information

ABSTRACT: A metal–organic supramolecular nanobelt was synthesized by quantitative self-assembling terpyridine-functionized tetraphenylethylene (TPE) and Cd^{2+}, which only showed a weak emission both in solution or aggregated state. Nevertheless, nanobelt complex could be transferred to a fluorescence turn-on sensor to S^{2-} by taking advantage of the structural transformation from nanobelt to its fluorescent ligand.

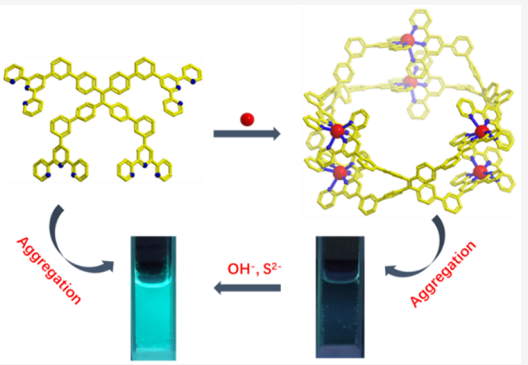

INTRODUCTION

Tetraphenylethene (TPE) was a typical aggregation-induced emission (AIE) luminogen, which was first put forward by Tang and colleagues,[1] and a variety of AIE materials based on TPE have been developed and utilized in various areas.[2−5] Facilitated by the highly directional and predictable feature of coordination-driven self-assembly, rationally incorporating TPE moiety to ligands is an alternative strategy to obtain a metal–organic supramolecular structure with desired optical properties.[6−11] There are two methods to construct such an assembled structure. One method is the anchoring of the TPE moiety on ligands as an attachment, in which the resultant metallo-assembly showed expected AIE properties.[12−14] The other is the use of the TPE unit as the rigid skeleton to generate the 2D and 3D supramolecular architecture.[5,7,15,16] By the subtle designing of the shape of ligand and assembled architecture, the resultant complexes showed unique emissive behavior due to the restriction of intramolecular rotation (RIR) resulting from the metal-coordination.[15,17] Recently, the pure white-light emission from a metallo-rosettes in both solution and aggregation states was developed by incorporating the TPE fluorophores.[12] Stang et al. found that the emissive behavior of supramolecular coordination complexes was affected by subtle structural factors, in which the fused rhomboid structure displayed a weaker fluorescence than the fused triangle in dilute solutions, while the result was reversed for the aggregated state.[18] All of above complexes showed intense emission in solution or in the aggregation state. But, obtaining the TPE-containing supramolecular aggregates in which ligands showed strong emission while the metallo-architecture was weak and/or not emissive was meaningful, because such a system could serve as fluorescent sensors resulting from the structural transformation. Further, the fact that the complexes in solid state were non-/weak-emissive facilitates the practical applications as fluorescent turn-on sensors, wherein responsive molecules exists in aggregation form.[19] Herein, the tetrapodal TPE-terpyridine ligands were synthesized and showed intense AIE effect. But, unexpectedly, the assembled metal–organic nanobelt and corresponding aggregates were weakly luminous. Based on these results, the nanoaggregates system was constructed and displayed obvious stimuli-responsive emission enhancement for S^{2-}.

RESULTS AND DISCUSSION

As shown in Scheme 1, tetrapodal ligand **L** was designed and synthesized utilizing the 4-fold Suzuki coupling of 1,1,2,2-tetrakis(4-bromophenyl)ethene and 4′-(4-boronatophenyl)-tpy. The structure of **L** was verified by ^{1}H NMR, in which a set of signals corresponding to terpyridine moiety was shown, including one characteristic singlet at 8.75 ppm assigned to the $H^{3',5'}$ and two doublets and two triplets attributed to the $H^{3,3''}$, $H^{6,6''}$ and $H^{4,4''}$, $H^{5,5''}$, respectively (Figure 1a).

Received: March 29, 2020

Scheme 1. Illustration of the Self-Assembly of Metal-Organic Nanobelt S

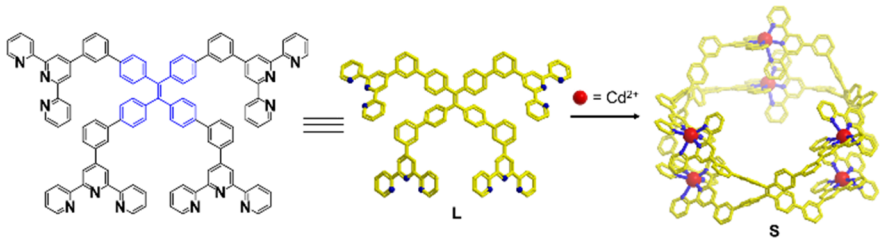

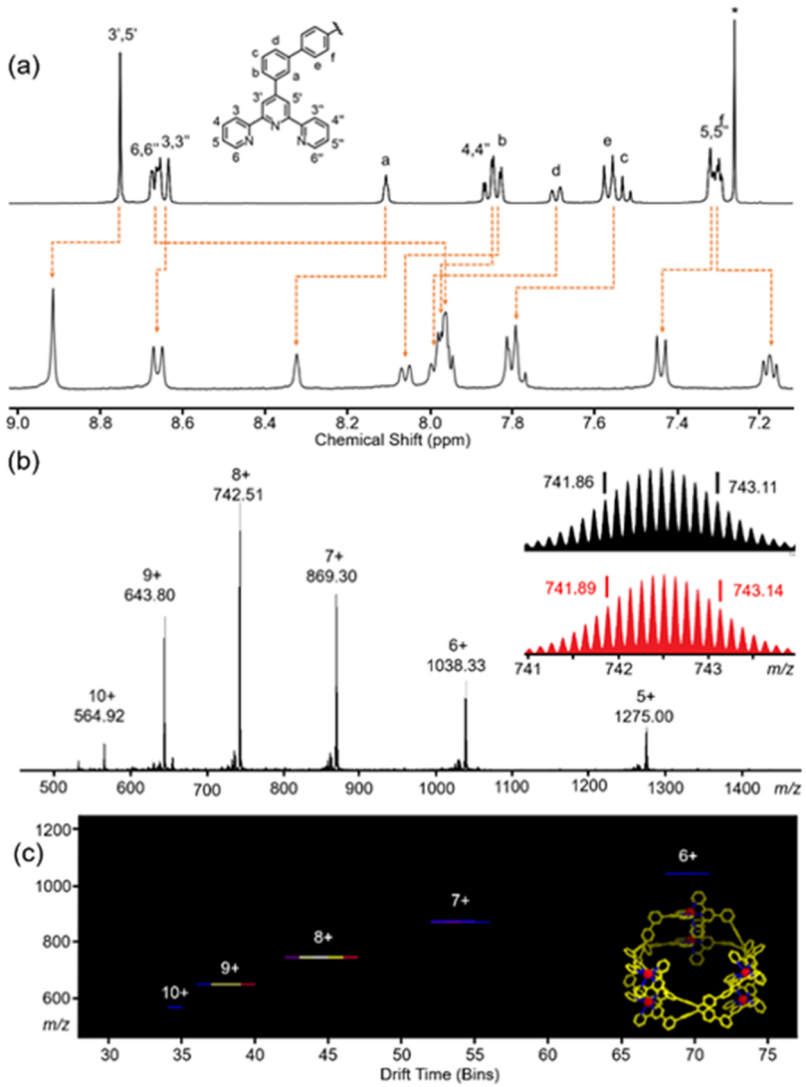

Figure 1. (a) ^{1}H NMR spectra (500 MHz) of **L** (top) in $CDCl_3$ (* for $CHCl_3$) and self-assembled nanobelt **S** (bottom) in CD_3CN. (b) ESI-MS and (c) 2D ESI-MS plot (m/z vs drift time) of **S**. The charge states of intact assemblies are marked, and the inset corresponds to energy-minimized structure.

Furthermore, the peak observed from electrospray ionization mass spectrum (ESI-MS) was found at 781.816 (cal. 781.809) contributed to $[M + 2H]^{2+}$, demonstrating the successful synthesis of ligand **L** (Figure S4).

The self-assembly of nanobelt was performed by mixing **L** and $Cd(NO_3)_2$ with a precise stoichiometric ratio (1:2) in $CHCl_3/CH_3OH$. After counterion exchange with PF_6^-, the nanobelt structure **S** was afforded in 93% yield (Scheme 1).

As shown in Figure 1a, the resultant assembled product was initially characterized by the NMR spectrum. In comparison to the ligand **L**, the resonance signals of complex **S** displayed clear change, in which the downfield-shift from 8.75 to 8.92 ppm of characteristic $tpyH^{3',5'}$ was clearly observed resulting from the electron-withdrawing effect upon coordination, and the dramatic upfield-shift from 8.67 to 7.92 ppm of $tpyH^{6,6''}$ was also distinctly observed owing to the electron shielding effect from metal ions.[20] Additionally, only one set of sharp proton signals of the terpyridine unit with an identical integrated ratio was displayed, demonstrating formation of single and discrete assembled structure. All of ^{1}H NMR peaks were fully assigned by means of correlated spectroscopy (2D COSY) (Figure S7).

https://dx.doi.org/10.1021/acs.inorgchem.0c00928
Inorg. Chem. XXXX, XXX, XXX−XXX

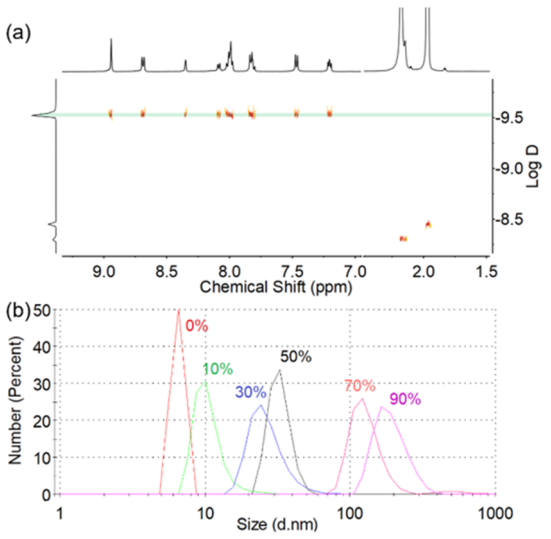

Figure 2. (a) DOSY spectrum of complex **S** in CD_3CN and (b) DLS datum of complex **S** in CH_3CN with various H_2O fractions (c = 7.04 × 10^{-6} M).

Further, the ESI-MS of complex **S** showed just a series of clear peaks with sequential charge states from 5+ to 10+ that contributed to the structure by losing different numbers of PF_6^- (Figure 1b). The experimental isotope patterns of each signal were in good accordance with the corresponding theoretical one, unambiguously supporting the composition of desired nanobelt $[L_3Cd_6]$ (Figure 1b, Figure S10). Importantly, the ESI-TWIM-MS, served as the 2D MS analysis, was used to verify the desired structure. As displayed in Figure 1c, the single species of charged signals (z = 6+ to 10+) with narrow drift time distributions was exclusively observed, indicative of the absence of any superimposed fragments or overlapping isomers or conformers. Derived from the ESI-TWIM-MS datum, an average collision cross section (CCS) was determined to be 808.97 ± 20.29 Å^2, which was coincident with the simulated results (Table S1).

More information for the size of the nanobelt structure **S** were obtained by the diffusion-ordered NMR spectroscopy (DOSY) and dynamic light scattering (DLS) experiments. All of the relevant signals of complex **S** in the DOSY spectrum were in a narrow band with the diffusion coefficient (D) of 3.02 × 10^{-10} m^2 s^{-1} (Figure 2a), indicating the creation of a single assembly. The dynamic radius was calculated to be 1.97 nm using the Stokes−Einstein equation, which consisted well with the sizes of energy-minimized structures from molecular modeling (Figure S11), demonstrating the formation of a desired nanobelt structure. Furthermore, the radius of nanobelt **S** was determined to be 3.2 nm from the DLS experiments (Figure 2b), which was also matched with the molecule structure.

The absorption spectrum of ligand **L** in dilute $CHCl_3$ showed an intense band centered at 280 nm with molar absorption coefficients (ε) of 1.27 × 10^5 M^{-1} cm^{-1} assigned to ligand-centered (LC) $\pi-\pi^*$ transitions (Figure 3a). In comparison with the ligand, the complex **S** in dilute MeCN has a more intense band at 287 nm with molar absorption

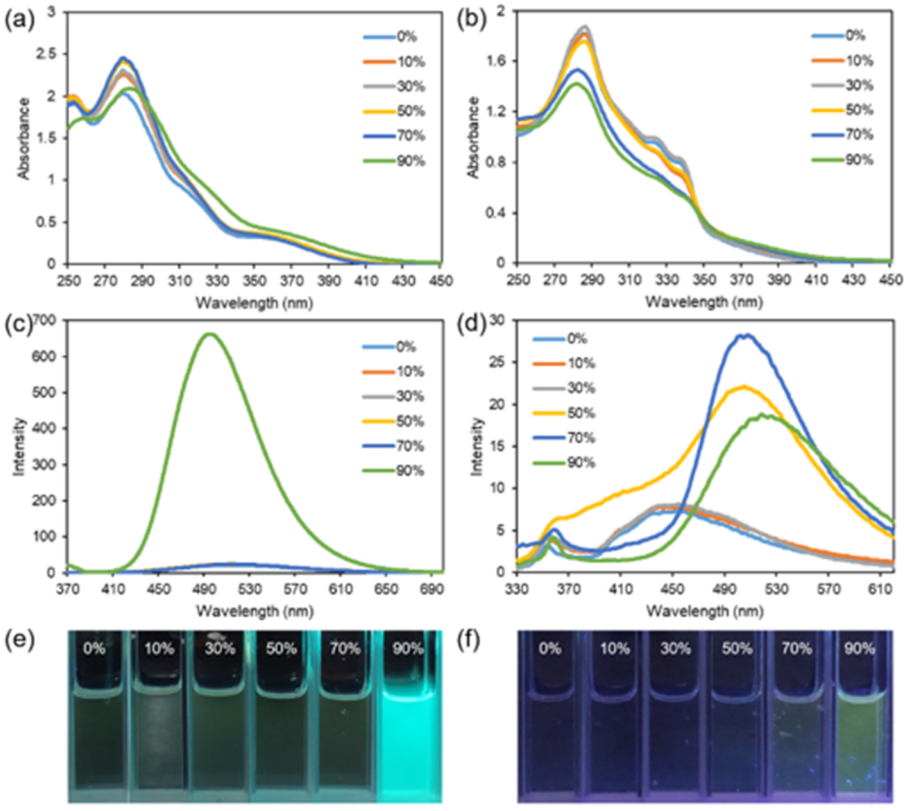

Figure 3. (a) UV−vis spectra, (c) fluorescence emission spectra (λ_{ex} = 360 nm; slit width: ex = 5 nm, em = 2.5 nm), and (e) photographs upon excitation at 365 nm of ligand **L** versus CH_3OH fraction in 2 mL $CHCl_3/CH_3OH$ mixtures (c = 1.6 × 10^{-5} M). (b) UV−vis spectrum, (d) fluorescence emission spectra (λ_{ex} = 320 nm; slit width: ex = 5 nm, em = 5 nm), and (f) photographs upon excitation at 365 nm of complex **S** versus H_2O fraction in 2 mL CH_3CN/H_2O mixtures (c = 7.04 × 10^{-6} M).

https://dx.doi.org/10.1021/acs.inorgchem.0c00928
Inorg. Chem. XXXX, XXX, XXX−XXX

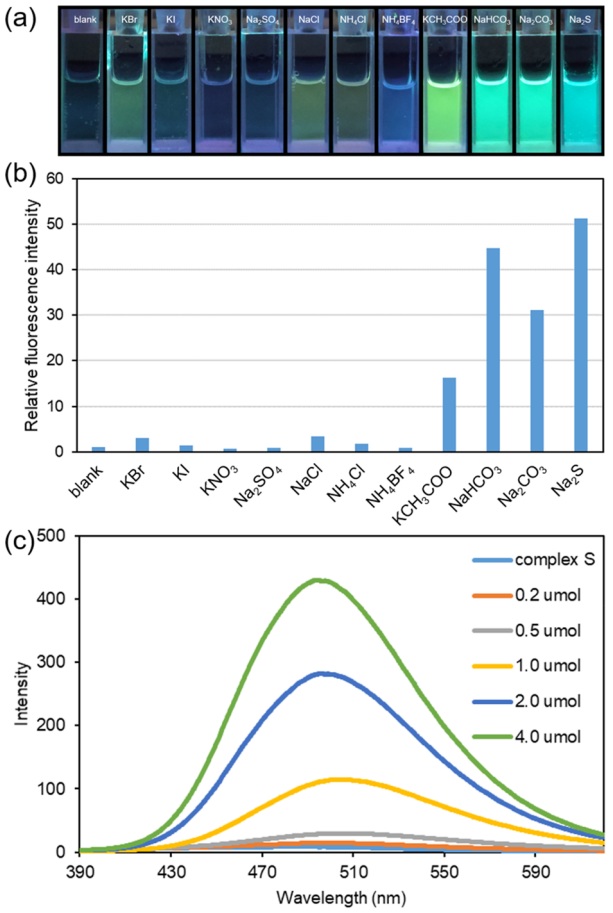

Figure 4. Fluorescence responses of complex **S** in 2 mL of CH_3CN/H_2O at 298 K (v/v, 1/1; $c = 7.04 \times 10^{-6}$ M): (a) the photographs (λ_{ex} = 365 nm) and (b) the relative fluorescence intensity of after and before addition of 4.0 μmol interfering species; c) fluorescence spectra after adding different concentrations of Na_2S (λ_{ex} = 320 nm; slit width: ex = 5 nm, em = 5 nm).

coeffucients (ε) of 2.57×10^5 M^{-1} cm^{-1} and two distinct absorption bands at ~322 and ~334 nm (Figure 3b), which are assigned to intraligand charge transfer (ILCT).[21] To further research the light-emitting behavior of ligand **L** and assembled nanobelt **S**, the UV−vis and fluorescence spectra were determined in mixed solvent with the different fraction of poor solvent. As shown in Figure 3c, Figure 3e, and Figure S13, the ligand **L** displayed weak luminescence in $CHCl_3$ and there was no obvious change with gradually increasing methanol or hexane fraction from 10% to 70% due to its solubility; however, the fluorescence intensities displayed obvious enhancement with 90% CH_3OH or hexane fraction. As we expected, such result was attributed to the AIE effect of TPE-containing **L**. As observed from Figure 3a and Figure S12, the formation of aggregates with 90% CH_3OH or hexane was verified by the decrease of high-energy bands at 283 nm and increase of low-energy tailing bands in the absorption spectra due to the $\pi-\pi$ stacking interactions.[22] Moving to complex **S**, which was nonluminescent in dilute CH_3CN, just a slight emission enhancement was observed with gradually increasing methanol or water fraction from 10% to 90% (Figure S15, Figure 3d, and Figure 3f). Surely, as observed from Figure 3f, the aggregates were obviously formed with 90% water, supported by the UV−vis spectra in which a similar change to the ligand was observed. Further, the aggregates forming was proved by the DLS results, in which the average hydrodynamic diameters (D_h) were measured to be 16, 24, 32, 122, and 164 nm with 10%, 30%, 50%, 70%, and 90% H_2O, respectively (Figure 2b). Tetraphenylethene (TPE) is a typical aggregation-induced emission (AIE) luminogen, which is nonemissive in solution but shows intense emission in aggregated state. Unexpectedly, complex **S** exhibited weak emission in aggregated state. Complex **S** possesses a rigid 3D structure by complexing with metal ions to form a nanobelt. We speculated that such rigid 3D structure of complex **S** hinders compact packing and the conformation of TPE units might not be intensely affected even in aggregated state, as a result to negligible AIE phenomenon.[23,24]

Tpy-Cd complexes were unstable and prone to disassemble to tpy ligands under alkaline conditions or S^{2-} existing due to the formation of insoluble cadmium salt. Based on this fact, herein, the aggregates of complex **S** were explored as a fluorescence turn-on sensor responsive to S^{2-}. Initially, fluorescence turn-on experiments were performed in CH_3CN/H_2O (v/v, 1/9) mixture, but the fluorescence intensity could not be accurately measured due to the fact that obvious precipitates were formed after adding analysts (Figure S17). Thus, the complex **S** in CH_3CN/H_2O (v/v, 1/1) mixture was chosen as the experimental subject, and the volume of each experiment was 2.0 mL. As described in Figure 4a, after 4.0 μmol of various salts (KBr, KI, KNO_3, Na_2SO_4, NaCl, NH_4Cl, NH_4BF_4, CH_3COOK, $NaHCO_3$, Na_2CO_3, Na_2S) was added to aggregates in CH_3CN/H_2O (v/v,1/1), complex **S** showed a specific emission enhancement response to alkali salt (CH_3COOK, $NaHCO_3$, Na_2CO_3) and Na_2S. Corresponding fluorescent emission spectroscopies showed a 16-, 45-, 31-, and 51-fold enhancement for analyst CH_3COOK, $NaHCO_3$, Na_2CO_3, and Na_2S, respectively. In contrast, no obvious fluorescence enhancement was found from other analysts, and the slight emission increase for Br^-, Cl^-, and I^- was probably resulting from further aggregation via partly disassembly lead by halogen ions coordination (Figure 4b).[25] Such results were supported by the UV−vis spectroscopies, in which no considerable change was observed for NO_3^-, SO_4^{2-}, and BF_4^- and where there was a decrease of high-energy bands at 283 nm and an increase of low-energy tailing bands for Br^-, Cl^-, and I^- (Figure S18). Further, the characteristic ILCT band around 330 nm was still observed for other analysts; however, it disappeared for $NaHCO_3$, Na_2CO_3, and Na_2S, demonstrating that complex **S** was disassembled to ligands (Figure S18). Further, the ^1H NMR spectra displayed that the signals assigned to complex **S** fully disappeared and that the ligand **L** was formed after adding Na_2S, suggesting that Na_2S was able to disassemble the complex to form the ligands (Figures S8 and S9).

As displayed in Figure S23, time-dependent fluorescence spectra of complex **S** with excess S^{2-} (4.0 umol) were recorded in 2.0 mL of CH_3CN/H_2O (1/1, v/v). As the reaction proceeded, the emission at 494 nm rapidly increased before 90 s elapsed. From 90 to 1100 s, the rate of fluorescence enhancement gradually decreases to close to 0 over time (Figure S24). Further, the concentration-dependent fluorescence enhancement was determined by fluorescence titration experiments (Figure 4c). Upon the progressive addition of Na_2S to complex **S** in 2.0 mL of CH_3CN/H_2O (1/1, v/v), the fluorescence intensity at 494 nm gradually increased. There was good linearity between the fluorescence intensity and the concentration of the Na_2S in the $0-1.0 \times 10^{-3}$ M range

https://dx.doi.org/10.1021/acs.inorgchem.0c00928
Inorg. Chem. XXXX, XXX, XXX−XXX

(Figure S22), supporting that complex **S** was a good candidate for quantitative detection of the S^{2-}.

CONCLUSION

In summary, an uncommon metal−organic supramolecular nanobelt was synthesized by the self-assembly of TPE-containing tetrapodal ligand with Cd^{2+}. As expected, the terpyridine ligands in aggregation state showed intense emission due to the AIE effect of TPE moieties; however, the complex **S** exhibited weak emission both in solution or in aggregates. Based on this fact, the complex **S** was developed as a fluorescence turn-on sensor to detect S^{2-} by taking advantage of the structural transformation from nanobelt **S** to ligand. These results impel us to further design and synthesize a more stable complex to withstand alkaline environments by using the suited metal ions and by improving the ligand dispersibility in H_2O by functional modification, as a result to obtain a new fluorescence probe to detect H_2S in vivo.

ASSOCIATED CONTENT

Supporting Information

The Supporting Information is available free of charge at https://pubs.acs.org/doi/10.1021/acs.inorgchem.0c00928.

Detailed synthetic protocols and characterization data for ligands and complexes (PDF)

AUTHOR INFORMATION

Corresponding Authors

Pingshan Wang − *Department of Organic and Polymer Chemistry; Hunan Key Laboratory of Micro & Nano Materials Interface Science, College of Chemistry and Chemical Engineering, Central South University, Changsha, Hunan 410083, China; Institute of Environmental Research at Greater Bay Area; Key Laboratory for Water Quality and Conservation of the Pearl River Delta, Ministry of Education; Guangzhou Key Laboratory for Clean Energy and Materials, Guangzhou University, Guangzhou 510006, China;* orcid.org/0000-0002-1988-7604; Email: chemwps@csu.edu.cn

Die Liu − *Institute of Environmental Research at Greater Bay Area; Key Laboratory for Water Quality and Conservation of the Pearl River Delta, Ministry of Education; Guangzhou Key Laboratory for Clean Energy and Materials, Guangzhou University, Guangzhou 510006, China*; Email: chem-ld@gzhu.edu.cn

Authors

Kaixiu Li − *Department of Organic and Polymer Chemistry; Hunan Key Laboratory of Micro & Nano Materials Interface Science, College of Chemistry and Chemical Engineering, Central South University, Changsha, Hunan 410083, China*

Zhengguang Li − *Department of Organic and Polymer Chemistry; Hunan Key Laboratory of Micro & Nano Materials Interface Science, College of Chemistry and Chemical Engineering, Central South University, Changsha, Hunan 410083, China*

Mingzhao Chen − *Institute of Environmental Research at Greater Bay Area; Key Laboratory for Water Quality and Conservation of the Pearl River Delta, Ministry of Education; Guangzhou Key Laboratory for Clean Energy and Materials, Guangzhou University, Guangzhou 510006, China*

Shi-Cheng Wang − *Department of Chemistry, National Taiwan University, Taipei 10617, Taiwan*

Yi-Tsu Chan − *Department of Chemistry, National Taiwan University, Taipei 10617, Taiwan;* orcid.org/0000-0001-9658-2188

Complete contact information is available at: https://pubs.acs.org/10.1021/acs.inorgchem.0c00928

Author Contributions

#K.L. and Z.L. contributed equally to this work.The manuscript was written through contributions of all authors. All authors have given approval to the final version of the manuscript.

Notes

The authors declare no competing financial interest.

ACKNOWLEDGMENTS

We acknowledge the support from the National Natural Science Foundation of China (21971257) and the Hunan Provincial Science and Technology Plan Project of China (2019TP1001). Y.-T.C. acknowledges the support from the Ministry of Science and Technology of Taiwan (MOST106-2628M-002-007MY3). The authors gratefully acknowledge the NMR spectroscopy measurements from the Modern Analysis and Testing Center of CSU.

REFERENCES

(1) Hong, Y.; Lam, J. W. Y.; Tang, B. Z. Aggregation-induced emission: phenomenon, mechanism and applications. *Chem. Commun.* **2009**, 4332−4353.

(2) Hong, Y.; Lam, J. W. Y.; Tang, B. Z. Aggregation-induced emission. *Chem. Soc. Rev.* **2011**, *40*, 5361−5388.

(3) Mei, J.; Leung, N. L. C.; Kwok, R. T. K.; Lam, J. W. Y.; Tang, B. Z. Aggregation-Induced Emission: Together We Shine, United We Soar! *Chem. Rev.* **2015**, *115*, 11718−11940.

(4) Zhang, M.; Li, S.; Yan, X.; Zhou, Z.; Saha, M. L.; Wang, Y.-C.; Stang, P. J. Fluorescent metallacycle-cored polymers via covalent linkage and their use as contrast agents for cell imaging. *Proc. Natl. Acad. Sci. U. S. A.* **2016**, *113*, 11100.

(5) Yan, X.; Cook, T. R.; Wang, P.; Huang, F.; Stang, P. J. Highly emissive platinum(II) metallacages. *Nat. Chem.* **2015**, *7*, 342−348.

(6) Zhang, M.; Saha, M. L.; Wang, M.; Zhou, Z.; Song, B.; Lu, C.; Yan, X.; Li, X.; Huang, F.; Yin, S.; Stang, P. J. Multicomponent Platinum(II) Cages with Tunable Emission and Amino Acid Sensing. *J. Am. Chem. Soc.* **2017**, *139*, 5067−5074.

(7) Yan, X.; Wang, H.; Hauke, C. E.; Cook, T. R.; Wang, M.; Saha, M. L.; Zhou, Z.; Zhang, M.; Li, X.; Huang, F.; Stang, P. J. A Suite of Tetraphenylethylene-Based Discrete Organoplatinum(II) Metallacycles: Controllable Structure and Stoichiometry, Aggregation-Induced Emission, and Nitroaromatics Sensing. *J. Am. Chem. Soc.* **2015**, *137*, 15276−15286.

(8) Jiang, B.; Zhang, C.-W.; Shi, X.-L.; Yang, H.-B. AIE-active Metal-organic Coordination Complexes Based on Tetraphenylethylene Unit and Their Applications. *Chin. J. Polym. Sci.* **2019**, *37*, 372−382.

(9) Zhang, C.-W.; Ou, B.; Jiang, S.-T.; Yin, G.-Q.; Chen, L.-J.; Xu, L.; Li, X.; Yang, H.-B. Cross-linked AIE supramolecular polymer gels with multiple stimuli-responsive behaviours constructed by hierarchical self-assembly. *Polym. Chem.* **2018**, *9*, 2021−2030.

(10) Zhang, T.; Zhang, G.-L.; Yan, Q.-Q.; Zhou, L.-P.; Cai, L.-X.; Guo, X.-Q.; Sun, Q.-F. Self-Assembly of a Tetraphenylethylene-Based Capsule Showing Both Aggregation- and Encapsulation-Induced Emission Properties. *Inorg. Chem.* **2018**, *57*, 3596−3601.

(11) Li, Y.; An, Y.-Y.; Fan, J.-Z.; Liu, X.-X.; Li, X.; Hahn, F. E.; Wang, Y.-Y.; Han, Y.-F. Strategy for the Construction of Diverse Poly-NHC-Derived Assemblies and Their Photoinduced Transformations. *Angew. Chem., Int. Ed.* **2019**, 1 DOI: 10.1002/anie.201912322.

(12) Chen, L.-J.; Ren, Y.-Y.; Wu, N.-W.; Sun, B.; Ma, J.-Q.; Zhang, L.; Tan, H.; Liu, M.; Li, X.; Yang, H.-B. Hierarchical Self-Assembly of Discrete Organoplatinum(II) Metallacycles with Polysaccharide via

Electrostatic Interactions and Their Application for Heparin Detection. *J. Am. Chem. Soc.* **2015**, *137*, 11725−11735.
(13) Yan, X.; Wei, P.; Liu, Y.; Wang, M.; Chen, C.; Zhao, J.; Li, G.; Saha, M. L.; Zhou, Z.; An, Z.; Li, X.; Stang, P. J. Endo- and Exo-Functionalized Tetraphenylethylene M12L24 Nanospheres: Fluorescence Emission inside a Confined Space. *J. Am. Chem. Soc.* **2019**, *141*, 9673−9679.
(14) Wang, Y.-S.; Bai, S.; Wang, Y.-Y.; Han, Y.-F. Process-tracing study on the post-assembly modification of poly-NHC-based metallosupramolecular cylinders with tunable aggregation-induced emission. *Chem. Commun.* **2019**, *55*, 13689−13692.
(15) Yin, G.-Q.; Wang, H.; Wang, X.-Q.; Song, B.; Chen, L.-J.; Wang, L.; Hao, X.-Q.; Yang, H.-B.; Li, X. Self-assembly of emissive supramolecular rosettes with increasing complexity using multitopic terpyridine ligands. *Nat. Commun.* **2018**, *9*, 567.
(16) Sun, L.-Y.; Feng, T.; Das, R.; Hahn, F. E.; Han, Y.-F. Synthesis, Characterization, and Properties of Tetraphenylethylene-Based Tetrakis-NHC Ligands and Their Metal Complexes. *Chem. - Eur. J.* **2019**, *25*, 9764−9770.
(17) Sun, Y.; Yao, Y.; Wang, H.; Fu, W.; Chen, C.; Saha, M. L.; Zhang, M.; Datta, S.; Zhou, Z.; Yu, H.; Li, X.; Stang, P. J. Self-Assembly of Metallacages into Multidimensional Suprastructures with Tunable Emissions. *J. Am. Chem. Soc.* **2018**, *140*, 12819−12828.
(18) Zhou, Z.; Yan, X.; Saha, M. L.; Zhang, M.; Wang, M.; Li, X.; Stang, P. J. Immobilizing Tetraphenylethylene into Fused Metallacycles: Shape Effects on Fluorescence Emission. *J. Am. Chem. Soc.* **2016**, *138*, 13131−13134.
(19) Thomas, S. W.; Joly, G. D.; Swager, T. M. Chemical Sensors Based on Amplifying Fluorescent Conjugated Polymers. *Chem. Rev.* **2007**, *107*, 1339−1386.
(20) Wang, J.-L.; Li, X.; Lu, X.; Hsieh, I. F.; Cao, Y.; Moorefield, C. N.; Wesdemiotis, C.; Cheng, S. Z. D.; Newkome, G. R. Stoichiometric Self-Assembly of Shape-Persistent 2D Complexes: A Facile Route to a Symmetric Supramacromolecular Spoked Wheel. *J. Am. Chem. Soc.* **2011**, *133*, 11450−11453.
(21) Chung, S.-K.; Tseng, Y.-R.; Chen, C.-Y.; Sun, S.-S. A Selective Colorimetric Hg2+ Probe Featuring a Styryl Dithiaazacrown Containing Platinum(II) Terpyridine Complex through Modulation of the Relative Strength of ICT and MLCT Transitions. *Inorg. Chem.* **2011**, *50*, 2711−2713.
(22) Leung, S. Y.-L.; Evariste, S.; Lescop, C.; Hissler, M.; Yam, V. W.-W. Supramolecular assembly of a phosphole-based moiety into nanostructures dictated by alkynylplatinum(ii) terpyridine complexes through non-covalent Pt···Pt and π-π stacking interactions: synthesis, characterization, photophysics and self-assembly behaviors. *Chem. Sci.* **2017**, *8*, 4264−4273.
(23) He, Y.-G.; Shi, S.-Y.; Liu, N.; Ding, Y.-S.; Yin, J.; Wu, Z.-Q. Tetraphenylethene-Functionalized Conjugated Helical Poly(phenyl isocyanide) with Tunable Light Emission, Assembly Morphology, and Specific Applications. *Macromolecules* **2016**, *49*, 48−58.
(24) Chan, C. Y. K.; Lam, J. W. Y.; Deng, C.; Chen, X.; Wong, K. S.; Tang, B. Z. Synthesis, Light Emission, Explosive Detection, Fluorescent Photopatterning, and Optical Limiting of Disubstituted Polyacetylenes Carrying Tetraphenylethene Luminogens. *Macromolecules* **2015**, *48*, 1038−1047.
(25) Šloufová, I.; Vlčková, B.; Mojzeš, P.; Matulková, I.; Císařová, I.; Procházka, M.; Vohlídal, J. Probing the Formation, Structure, and Reactivity of Zn(II), Ag(I), and Fe(II) Complexes with 2,2′:6′,2″-Terpyridine on Ag Nanoparticles Surfaces by Time Evolution of SERS Spectra, Factor Analysis, and DFT Calculations. *J. Phys. Chem. C* **2018**, *122*, 6066−6077.

https://dx.doi.org/10.1021/acs.inorgchem.0c00928
Inorg. Chem. XXXX, XXX, XXX−XXX